Atmospheric Pollution Research 8 (2017) 439–445

Contents lists available at ScienceDirect

Atmospheric Pollution Research

journal homepage: http://www.journals.elsevier.com/locate/apr

# Influence of emission rate on atmospheric dispersion modeling of the Fukushima Daiichi Nuclear Power Plant accident

Xiaobing Geng [a, b], Zhenghui Xie [a, *], Lijun Zhang [b]

[a] Institute of Atmospheric Physics, Chinese Academy of Sciences, P.O.Box 9804, Beijing 100029, China
[b] Institute of Chemical Defence, P.O.Box 1048, Beijing 102205, China

ARTICLE INFO

*Article history:*
Received 19 August 2016
Received in revised form
27 October 2016
Accepted 31 October 2016
Available online 24 November 2016

*Keywords:*
Fukushima accident
Atmospheric dispersion modeling
FLEXPART-WRF
Source term
Airborne nuclear release

ABSTRACT

The role of emission rate in atmospheric dispersion modeling was investigated in this study. Six different emission rates that were estimated by the Japan Atomic Energy Agency and Norwegian Institute for Air Research after the Fukushima Daiichi Nuclear Power Plant accident were used as inputs to FLEXPART-WRF, a Lagrangian particle dispersion model. High-resolution (1 km) meteorological data in a local scale region (100 km) were downscaled dynamically by the Weather Research and Forecasting model from a reanalysis of ERA-Interim during 11–31 March, 2011, and were used to drive the model. The accumulated deposition of $^{137}$Cs was used to assess the simulations. Deposition occurred mainly during four periods dominated by wet deposition due to precipitation, which were 15, 20–22, 25, and 30–31 March. The basic deposition pattern was established on 15 March, shortly after the highest emission rates of 14 March, and the largest variation in deposition with the different emission rates was also observed in this period. Emission rates estimated are usually not independent from the models and meteorological input data. The model-meteorology combination used for emergency response activities had better be the one used to determine the source term.



## 1. Introduction

The accidental release of radioactive material from nuclear power plants can cause serious environmental problems, as shown by the Fukushima Daiichi Nuclear Power Plant (FDNPP) and Chernobyl accidents. In recent years, the results of atmospheric transport, dispersion, and deposition models (ATDMs) have been used to estimate the full extent of pollution, radiological monitoring, and planning for countermeasures, especially during the early stages of such nuclear emergencies (Benamrane et al., 2013). ATDMs can be used to predict where the release is most likely to be deposited, and thus which areas could be affected and how serious the contamination could be in near real-time.

Model predictions are influenced by the particular ATDM used, meteorological data, and the source term (emission rates in this study) (Benamrane et al., 2013; Arnold et al., 2015). The numerical schemes and parameterizations of several ATDMs (WSPEEDI (Katata et al., 2015), FLEXPART (Arnold et al., 2015), MLDP, and RATM (Draxler et al., 2015)) have been revised to obtain better simulations after the FDNPP accident. Arnold (Arnold et al., 2015) studied the influence of meteorological inputs on atmospheric dispersion modeling. However, to understand the atmospheric dispersion processes and assess radiological doses to the public, it is necessary to estimate the source term of the radionuclides during the accident. Thus, efforts to estimate and revise the source term by coupling atmospheric dispersion simulations and environmental monitoring data have been made by researchers around the world (Chino et al., 2011; Katata et al., 2012; Kobayashi et al., 2013; Stohl et al., 2012; Terada et al., 2012; Saunier and Mathieu, 2013; Winiarek et al., 2014).

As far as source term is concerned, some questions still need to be answered. For example, for the same case, what is the impact on modeling results of using different emission rates as an input, what factors control this impact, and how to get a better simulation? There are two reasons why these issues have not been addressed: the lack of a persuasive case and the lack of different source terms for the same case. The dispersion and deposition of radionuclides

* Corresponding author.
*E-mail address:* zxie@lasg.iap.ac.cn (Z. Xie).
Peer review under responsibility of Turkish National Committee for Air Pollution Research and Control.

http://dx.doi.org/10.1016/j.apr.2016.10.013
1309-1042/

after the FDNPP accident were very complicated (Benamrane et al., 2013) due to the number and duration of events (explosions, venting), rapid changes in weather conditions, and the complex topography around the FDNPP area. From this perspective, the accident is not an ideal test case (Arnold et al., 2015). However, some valuable data can be obtained by using a series of source terms for the same real case, which makes the FDNPP accident an unprecedented case to study source term sensitivity.

The objective of this study was to analyze the sensitivity of the source term in atmospheric dispersion modeling, using the FDNPP accident as a case study. High-resolution flow field simulations were conducted with the nested Weather Research and Forecasting (WRF)-Advanced Research WRF (ARW) mesoscale model at a range of 100 km around the site, followed by dispersion simulations using the flexible particle (FLEXPART) Lagrangian particle dispersion model (LPDM), with the available source term inputs. Simulations conducted by the World Meteorological Organization (WMO) Technical Task Team (TT) on Meteorological Analyses for the FDNPP accident (Draxler et al., 2013) were adopted for further analysis. In this report, the details of the methods and numerical simulations are first described and then the results are presented.

## 2. Methods

The sensitivity analysis was undertaken based on simulated deposition from 11 to 31 March, with validation using measurements in a region that extended for 100 km around the FDNPP. The details of the numerical simulations are given below.

### 2.1. Downscaling of reanalysis

High-resolution meteorological data are necessary to drive ATDMs to simulate detailed deposition at the local scale. However, reanalysis such as ERA-40 (Uppala et al., 2005) and ERA-Interim (Berrisford et al., 2011) from the European Centre for Medium Range Forecasts or the final analysis from the National Centers for Environmental Prediction have horizontal resolutions that are far too coarse for this application. Therefore, dynamical downscaling (Lo et al., 2008), a nested modeling approach, was used to obtain high-resolution local meteorological information from reanalysis data.

The WRF model (Skamarock et al., 2008) is a nonhydrostatic, compressible model that can simulate three-dimensional wind, potential temperature, geo-potential, surface pressure, turbulent kinetic energy, and moisture. It was designed as a numerical weather prediction model, and was applied for downscaling of reanalysis in this study.

A multi-scale simulation was performed using four two-way interactive nested domains (Fig. 1), with horizontal resolutions of 9, 3, and 1 km. To obtain realistic meteorological data for dispersion modeling, a sequence of 11 simulations was conducted with the ARW mesoscale model, each with 48-h integration, followed by a simulation with 24-h integration. This covered the significant 21-day release period from 11 to 31 March, 2011. The initial and boundary conditions for each simulation were derived from the ERA-Interim data on $0.125^\circ \times 0.125^\circ$ grids every 6 h. The model grid configuration and physics options are given in Table 1, and were validated by Srinivas (Srinivas and Venkatesan, 2012). Time-varying three-dimensional meteorological fields at 1-h intervals from the third domain were used in the dispersion simulations.

### 2.2. Atmospheric dispersion simulations

#### 2.2.1. Model configuration

A Lagrangian particle dispersion model, FLEXPART-WRF (Brioude et al., 2013), was used to simulate the atmospheric transport and dispersion of the accidental releases from FDNPP. The model enables the mesoscale transport, diffusion, and removal by dry and wet deposition, as well as the radioactive decay of radionuclides to be simulated.

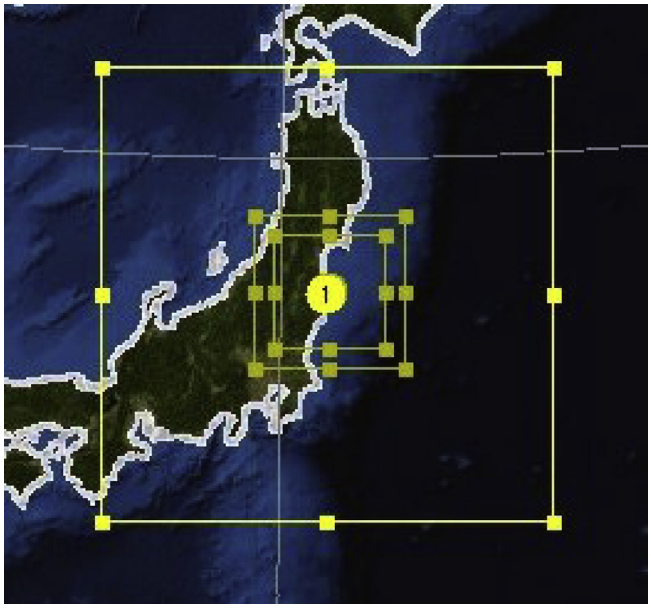


**Fig. 1.** Advanced Research (Weather Research and Forecasting: WRF) (ARW) simulation domains.

The computational grid size of FLEXPART-WRF was set to be the same as that of WRF. A total of 4200 pseudo-particles were released each hour. By dumping particle information at the end of each day, 21 simulations were relayed from 11 to 31 March. Each simulation was performed using three-hourly emission rates, driven by hourly WRF outputs.

The parameters used (Stohl et al., 2005) in the dry deposition of $^{137}Cs$ were as follows: density $\rho$ ($2.5 \times 10^3$ kg m$^{-3}$), mean particle diameter $d_p$ (0.6 $\mu$m), and standard deviation about mean size $\sigma_p$ ($3.0 \times 10^{-1}$ $\mu$m). The parameters used in wet deposition were the scavenging coefficient $A$ ($1.0 \times 10^{-4}$ s$^{-1}$) for a precipitation rate of 1 mm/h and rain rate dependency factor $B$ (0.80). The sampling rate was 180 s and the sampling average was 3600 s.

#### 2.2.2. Emission rates

Two methods have been used for estimating the source term of radionuclides discharged into the atmosphere, which are referred to as the reverse and the inverse. The reverse method simply calculates the emission rates of radionuclides (Bq h$^{-1}$) by coupling the atmospheric dispersion simulation with environmental monitoring data under the assumption of a unit emission rate (1 Bq h$^{-1}$) (Katata et al., 2015). The emission rates are estimated as the ratio of the monitoring data to the dispersion calculation. Most published emission rates (listed in Table 2) are obtained in this way. The first estimation of emission rates was performed by Chino et al. (2011). (hereinafter chino2011) using the System for Prediction of Environmental Emergency Dose Information (SPEEDI) and its worldwide version (WSPEEDI-II), which were modified by Terada et al. (2012). (hereinafter terada2012), and further revised by Fischer (Draxler et al., 2013) (hereinafter wmo2012). Kobayashi et al (Srinivas and Venkatesan, 2012). (hereinafter kobayashi2013) estimated a new source term using both atmospheric and oceanic dispersion models. A more detailed source term was estimated by Katata et al. (2015). (hereinafter katata2015), with more monitoring

**Table 1**
Details of the Weather Research and Forecasting (WRF) configuration.

| Dynamics | Primitive equations |
|---|---|
| Horizontal resolution | Domain 1—9 km (109 × 109)<br>Domain 2—3 km (109 × 109)<br>Domain 3—1 km (217 × 217) |
| Vertical levels | 40 |
| Domain center | 37.4026°N; 141.033°E |
| Model physics | Shortwave radiation: Dudhia scheme<br>Longwave radiation: Rapid Radiative Transfer Model (RRTM) scheme<br>Surface physics: NOAH land surface model (LSM<br>Planetary boundary layer (PBL): YonSei University (YSU) nonlocal diffusion<br>Convection: Kain-Fritsch<br>Microphysics: WSM3 class simple ice scheme |
| Initial/boundary conditions | ERA-Interim 0.125° × 0.125° analysis, every 6 h |

**Table 2**
Emission rates used in this article.

| Source term code | Observation station | Model | Method | Total emission of Cs137 before 20110401/PBq |
|---|---|---|---|---|
| chino2011 | land | SPEEDI + WSPEEDI-II | reverse | 13.2 |
| stohl2012 | land | FLEXPART | inverse | 35.1 |
| terada2012 | land | WSPEEDI-II | reverse | 14.2 |
| kobayashi2013 | land + ocean | WSPEEDI-II (atmospheric)<br>SEA-GEARN-FDM (oceanic) | reverse | 13.3 |
| katata2015 | land + ocean | WSPEEDI-II revised (atmospheric)<br>SEA-GEARN-FDM (oceanic) | reverse | 14.2 |
| wmo2012 | | | reverse | 12.5 |

data and using a more sophisticated model. The inverse estimation method (Katata et al., 2015) evaluates the emission rates in an objective way using an algorithm to minimize the differences between calculated and measured air concentrations or dose rates. Stohl et al. (2012) (hereinafter stohl2012) estimated a source term using this method, with FLEXPART.

All of the six source terms mentioned above are listed in Table 2. The time-varying emission rates are shown in Fig. 2, with emission rates varying rapidly between 11 and 16 March. Similarities between source terms were apparent. Two source terms, terada2012 (green line) and wmo2012 (brown line), are identical after 17 March, and so is kobayashi2013 (blue line) after 20 March. The source term of stohl2012, which was estimated by the inverse method, was smoother, while the others estimated by the reverse method varied abruptly. All of the six source terms were split into 3-h intervals and were used as inputs to FLEXPART-WRF.

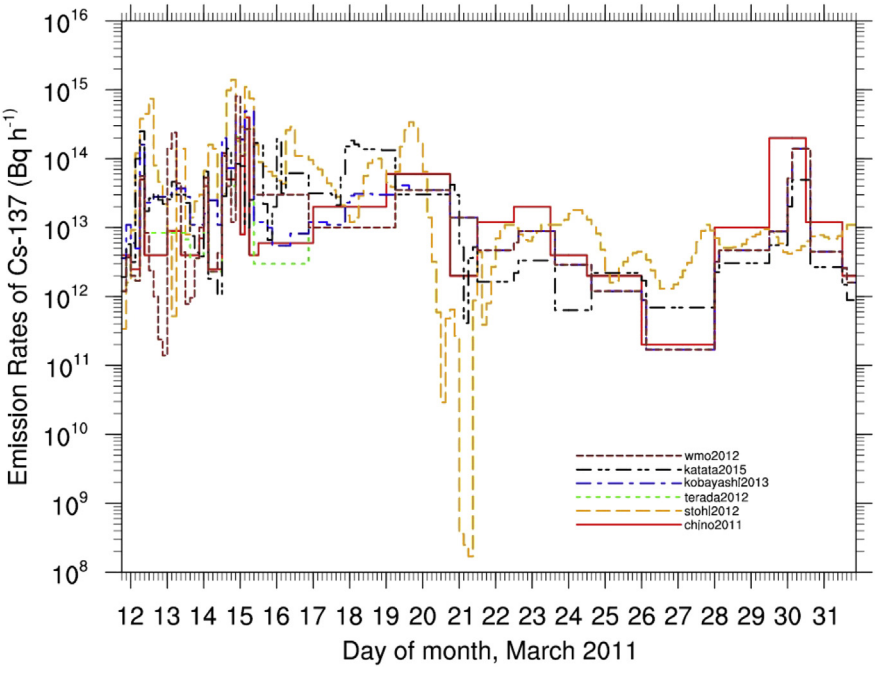


**Fig. 2.** Emission rates of $^{137}$Cs.

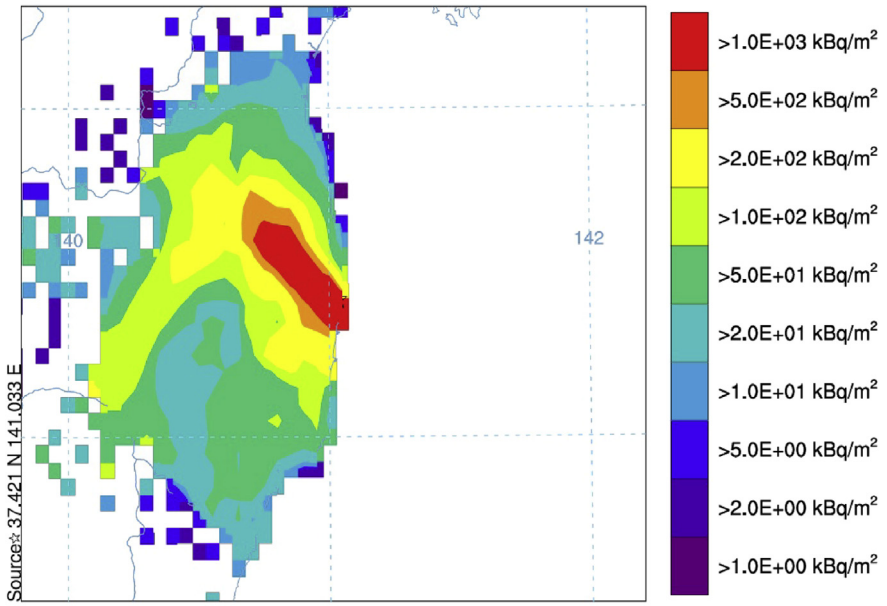


**Fig. 3.** Gridded digital map of $^{137}$Cs deposition on 31 March 2011, redrawn with data from http://ready.arl.noaa.gov/fdnppwmo/C137_deposit.txt.

*2.2.3. Observations*

During the FDNPP accident, data were collected for gamma dose rate, air concentration, and the accumulated deposition of certain radionuclides. Large amounts of gamma dose rate data are rarely used for the validation of ATDMs because they depend on the existing knowledge of chemical species and previously accumulated deposition data, which are not handled easily. Under the special circumstances of the FDNPP accident, air concentration data were available at only a few locations. Digital versions of $^{137}$Cs deposition maps on 31 March 2011 (Fig. 3) were available publicly. These were generated by merging airborne measurements by the U.S. Department of Energy's fixed-wing aircraft and ground-based measurements by the Ministry of Education, Culture, Sports and Science and Technology (MEXT). The gridded data consisted of 543 values, with a resolution of 0.05°. This data set was assumed to be the ground truth for $^{137}$Cs deposition and has been used for the validation of many simulations (Draxler et al., 2013, 2015).

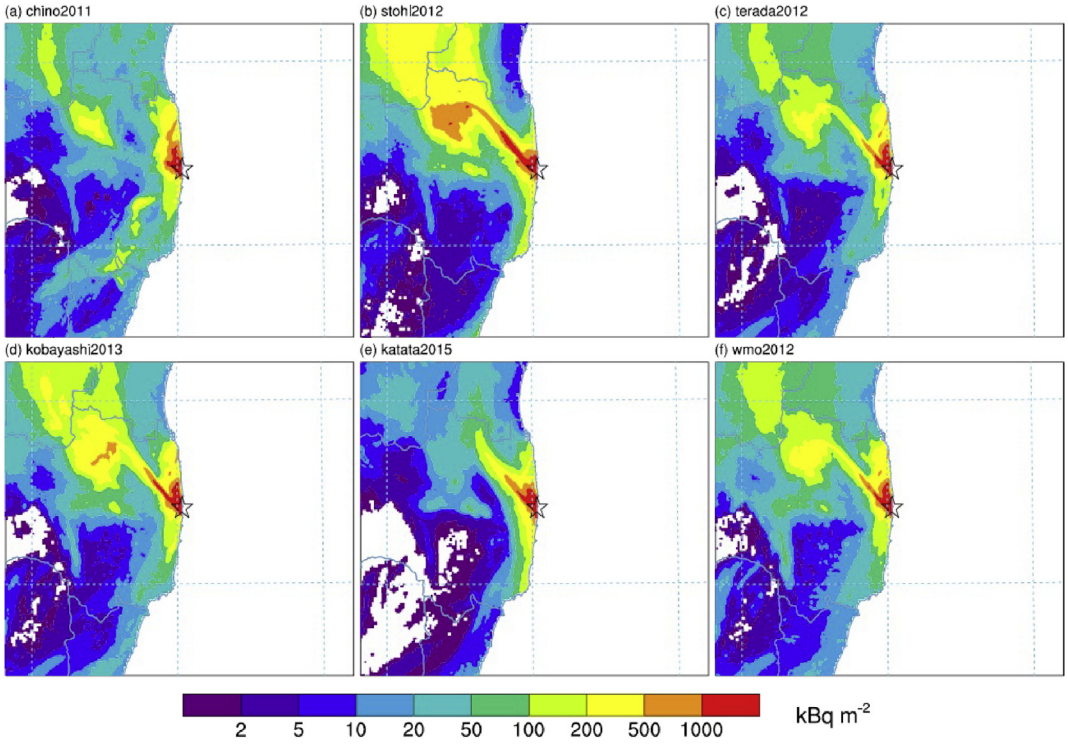


**Fig. 4.** Simulated deposition activity on April 1 (0000h).

**Table 3**
Atmospheric transport, dispersion, and deposition model (ATDM) performance for the total $^{137}$Cs deposition.

| Source term | CC | NMSE | FB | FMS | KSP |
|---|---|---|---|---|---|
| chino2011 | 0.02 | 24.13 | −0.60 | 100 | 25.41 |
| stohl2012 | **0.21** | **15.22** | **−0.27** | **100** | **22.47** |
| terada2012 | 0.09 | 26.32 | −0.78 | 100 | 35.17 |
| kobayashi2013 | 0.13 | 20.85 | −0.57 | 100 | 29.97 |
| katata2015 | 0.13 | 24.89 | −0.80 | 100 | 35.91 |
| wmo2012 | 0.09 | 24.51 | −0.64 | 100 | 27.44 |

## 3. Results and discussion

Simulated deposition maps for 1 April, 2011, for each of the six emission rates above are shown in Fig. 4. All six results indicated two rough areas of deposition. One was northwest of FDNPP and the other was along the coastline. The differences were significant. Of all six deposition results, the range (orange and yellow in the plots) of stohl2012 was the widest and its level of deposition was the highest. The deposition patterns of chino2011 and katata2015 were distinct from those of the other four. The deposition patterns of terada2012, wmo2012, and kobayashi2013 were almost the same despite the slightly different emission levels.

Considering that the same model and meteorological field were used, the above results can only be explained from the perspective of sources, namely, emission rates in this study. Among the six source terms investigated, chino2011 was the preliminary estimate and katata2015 was the latest available term, and both produced clearly different results than the other four terms. In contrast, chino2012, terada2012, and wmo2012 were retrieved using the same model with the same method. They have been gradually revised as more observations have become available. It is therefore not surprising that the deposition patterns that they produced were similar. Although the use of stohl2012 also produced a similar pattern, it was obtained using a different method with a different model.

To evaluate the ATDM simulations objectively, statistical parameters were investigated and the procedure of Draxler et al. (2015, 2013). was adopted. Five parameters were selected to represent different evaluation metrics: the correlation coefficient (CC), the normalized mean square error (NMSE), the fractional bias (FB), the figure-of-merit in space (FMS), and the Kolmogorov-Smirnov parameter (KSP). The performance of the six ATDMs for $^{137}$Cs is listed in Table 3. The bold highlight shows the emission rate with the best performance for each metric. The best performance over all of the metrics was obtained for stohl2012.

### 3.1. Deposition during key periods

To reveal how the deposition evolved over time, simulations were conducted with a unit emission rate. Fig. 5 shows the percentage of the total deposition of $^{137}$Cs for a unit emission rate (1 Bq h$^{-1}$), for the period to the end of March due to each 3-h source period. The area under this line adds up to 100%, that is, the entire simulated deposition in the region of interest (ROI). Four distinct periods were apparent when using this normalized deposition value: 15, 20–22, 25, and 30–31 March.

Deposition during each day in these periods is shown in Fig. 6 and Figs. S1–S6. It was evident that most of the released $^{137}$Cs was deposited during these periods. This also implies that the deposition results during these periods were particularly sensitive to any change in the emission rates. According to the simulated meteorological fields, winds blew towards the land and most precipitation occurred during these periods. The basic deposition pattern was formalized on the days of 15 and 30 March, with higher emission rates during these periods. The deposition on 20–22, 25, and 31 March added some further detail. The most contaminated area (northwest of the FDNPP) was the result of deposition on 15, 20, 22, and 25 March. The area of contamination along the coastline was formed on 30 March. Deposition on 21 and 31 March added some detail to the area southwest of the FDNPP.

### 3.2. Deposition on 15 March, 2011

To understand what caused the differences in deposition, it was necessary to analyze the basic deposition pattern formed on 15 March. The deposition results on this day for the six different emission rates are shown in Figs. S7–S14 in three-hourly sequential intervals. It can be seen that the radionuclides were deposited clockwise from southwest to north, with clear differences during each 3-h interval. The most contaminated region formed before 1200 northwest of FDNPP. The areas of deposition produced by using the chino2011 and katata2015 source terms were smaller than for the others. The largest area of contamination was projected when using stohl2012 because the area under the orange line during this period in Fig. 2 is the largest, and the amount of $^{137}$Cs released was also larger than for the other source terms.

### 3.3. Wet deposition and dry deposition

Precipitation is known to play an important role in deposition. Deposition in each 3-h interval in the ROI is shown in Fig. 7, and is shown as dry deposition (red line), wet deposition (blue line), and

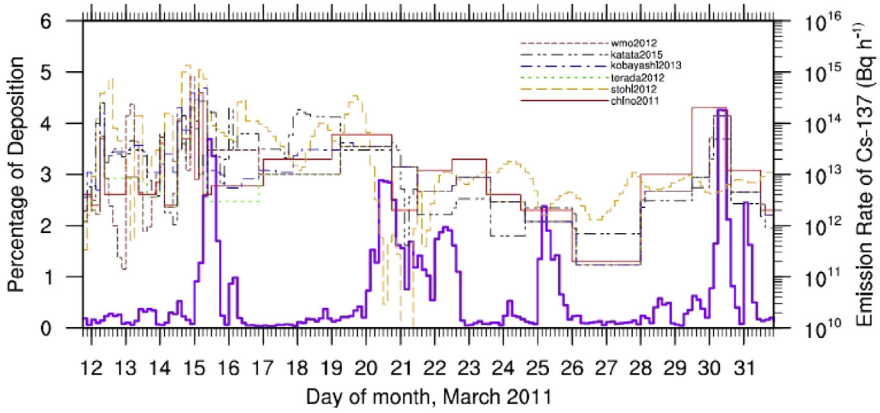


**Fig. 5.** Time evolution of the percentage of total deposition from 2011031118 to 2011040100 in the region of interest, assuming that emission rate of all sources was 1 Bq h$^{-1}$, compared to all the 6 emission rates.

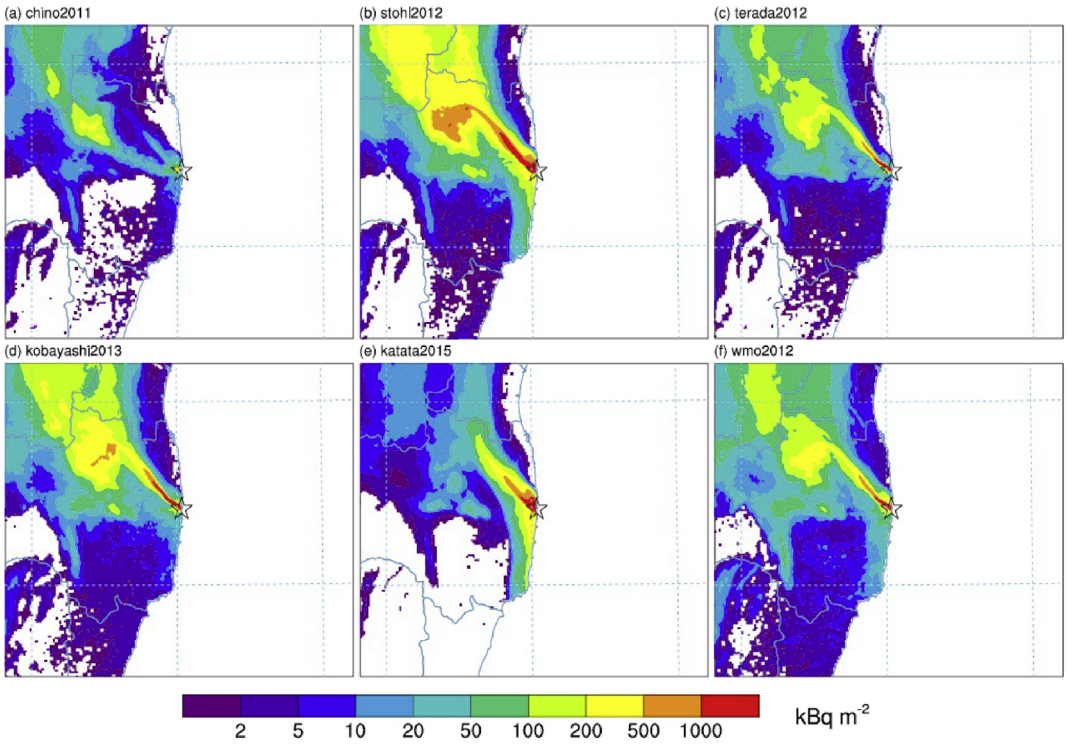


**Fig. 6.** Deposition on 15 March.

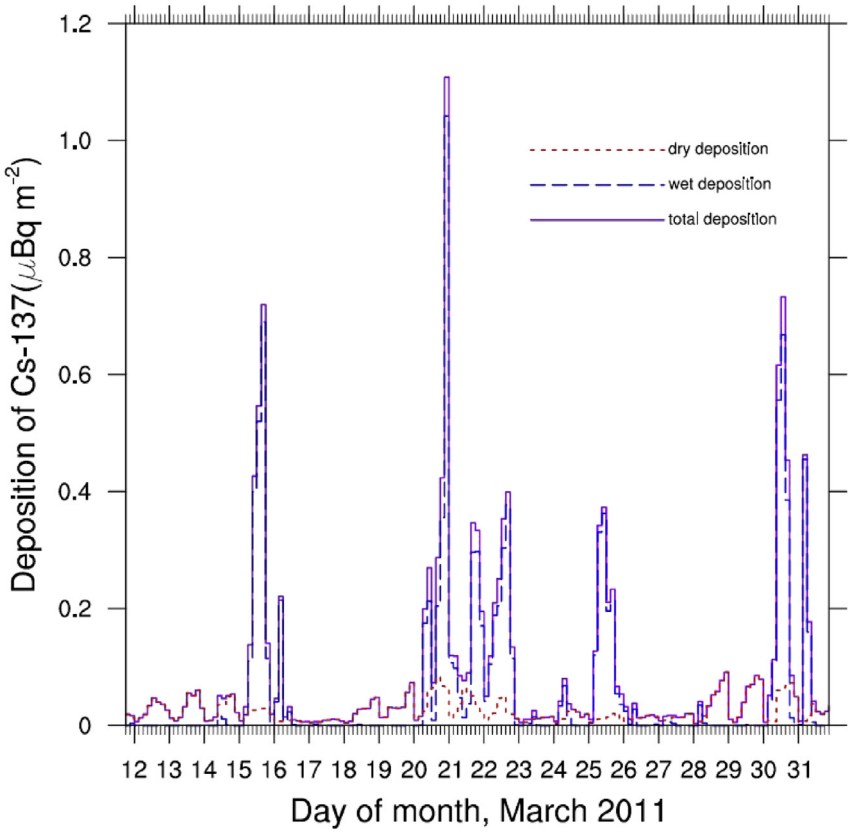


**Fig. 7.** Wet deposition vs. dry deposition.

both (purple line). During the key periods mentioned above, wet deposition dominates the cumulative surface activities. In the 21 days from 11 to 31 March, the fluctuations in dry deposition were relatively small. Therefore, the FDNPP accident can be considered an appropriate case to test the wet deposition schemes of different atmospheric dispersion models. The wet deposition schemes of many ATDMs were revised after this accident. Compared with old models, the shape of the most contaminated area of the new model (Katata et al., 2015) is similar to the shape of the number '7′, which matches the observed pattern.

## 4. Conclusions

To understand the influence of a time-varying source term in an ATDM, $^{137}$Cs deposition for a real case in the region 100 km around the FDNPP from 11 to 31 March, 2011, was simulated using FLEXPART-WRF with different emission rates.

Deposition occurred during four periods, 15, 20–22, 25, and 30–31 March, with precipitation and wind blowing towards the land. Wet deposition due to precipitation dominated the total deposition during these periods. The basic deposition pattern formed on 15 March, shortly after the highest emissions on 14 March.

The projected deposition using different source terms was different. The largest variation in deposition with the different emission rates was also observed on 15 March. The deposition closest to the observed pattern was obtained using stohl2012. The same ATDM-meteorology combination used to retrieve the source term produces the best simulation results for the same source term.

Emission rates estimated are usually not independent from the models and meteorological input data. The model-meteorology combination used for emergency response activities had better be the same used to determine the source term.

## Appendix A. Supplementary data

Supplementary data related to this article can be found at http://dx.doi.org/10.1016/j.apr.2016.10.013.

## References


Arnold, D., Maurer, C., Wotawa, G., Draxler, R., Saito, K., Seibert, P., 2015. Influence of the meteorological input on the atmospheric transport modelling with FLEXPART of radionuclides from the Fukushima Daiichi nuclear accident. J. Environ. Radioact. 139, 212–225. http://dx.doi.org/10.1016/j.jenvrad.2014.02.013.

Benamrane, Y., Wybo, J., Armand, P., 2013. Chernobyl and Fukushima nuclear accidents: what has changed in the use of atmospheric dispersion modeling? J. Environ. Radioact. 126, 239–252. http://dx.doi.org/10.1016/j.jenvrad.2013.07.009.

Berrisford, P., Dee, D., Poli, P., Brugge, R., Fielding, K., Fuentes, M., Kållberg, P., Kobayashi, S., Uppala, S., Simmons, A., November 2011. The Era-interim Archive Version 2.0. Shineld Park, Reading.

Brioude, J., Arnold, D., Stohl, A., 2013. The Lagrangian particle dispersion model FLEXPART-WRF version 3.1. Geosci. Model Dev. 6 (6), 1889–1904. http://dx.doi.org/10.5194/gmd-6-1889-2013.

Chino, M., Nakayama, H., Nagai, H., Terada, H., Katata, G., Yamazawa, H., 2011. Preliminary estimation of release amounts of $^{131}$I and $^{137}$Cs accidentally discharged from the Fukushima Daiichi nuclear power plant into the atmosphere. J. Nucl. Sci. Technol. 48, 1129–1134. http://dx.doi.org/10.1080/18811248.2011.9711799.

Draxler, R., Arnold, D., Galmarini, S., Hort, M., Jones, A., Leadbetter, S., Malo, A., Maurer, C., Rolph, G., Saito, K., Servranckx, R., Shimbori, T., Solazzo, E., Wotawa, G., December 2013. Evaluation of Meteorological Analyses for the Radionuclide Dispersion and Deposition from the Fukushima Daiichi Nuclear Power Plant Accident. Tech. rep.. World Meteorological Organization.

Draxler, R., Arnold, D., Chino, M., Galmarini, S., Hort, M., Jones, A., Leadbetter, S., Malo, A., Maurer, C., Rolph, G., Saito, K., Servranckx, R., Shimbori, T., Solazzo, E., Wotawa, G., 2015. World Meteorological Organization's model simulations of the radionuclide dispersion and deposition from the Fukushima Daiichi nuclear power plant accident. J. Environ. Radioact. 139, 172–184. http://dx.doi.org/10.1016/j.jenvrad.2013.09.014.

Katata, G., Ota, M., Terada, H., Chino, M., Nagai, H., Katata, G., Chino, M., Nagai, H., 2012. Atmospheric discharge and dispersion of radionuclides during the Fukushima Daiichi Nuclear Power Plant accident. Part I: source term estimation and local-scale atmospheric dispersion in early phase of the accident. J. Environ. Radioact. 109, 141–154. http://dx.doi.org/10.1016/j.jenvrad.2012.02.006.

Katata, G., Chino, M., Kobayashi, T., Terada, H., Ota, M., Nagai, H., Kajino, M., Draxler, R., Hort, M.C., Malo, A., Torii, T., Sanada, Y., 2015. Detailed source term estimation of the atmospheric release for the Fukushima Daiichi Nuclear Power Station accident by coupling simulations of an atmospheric dispersion model with an improved deposition scheme and oceanic dispersion model. Atmos. Chem. Phys. 15 (2), 1029–1070. http://dx.doi.org/10.5194/acp-15-1029-2015.

Kobayashi, T., Nagai, H., Chino, M., Kawamura, H., 2013. Source term estimation of atmospheric release due to the Fukushima Daiichi Nuclear Power Plant accident by atmospheric and oceanic dispersion simulations. J. Nucl. Sci. Technol. 50, 255–264. http://dx.doi.org/10.1080/00223131.2013.772449.

Lo, J.C.-F., Yang, Z.-L., Pielke, R.A., 2008. Assessment of three dynamical climate downscaling methods using the Weather Research and Forecasting (WRF) model. J. Geophys. Res. 113, D09112. http://dx.doi.org/10.1029/2007JD009216 (D9).

Saunier, O., Mathieu, A., 2013. An inverse modeling method to assess the source term of the Fukushima Nuclear Power Plant accident using gamma dose rate observations. Atmos. Chem. Phys. 13, 11403–11421. http://dx.doi.org/10.5149/acp-13-11403-2013.

Skamarock, W., Klemp, J., Dudhi, J., Gill, D., Barker, D., Duda, M., Huang, X.-Y., Wang, W., Powers, J., 2008. A Description of the Advanced Research WRF Version 3. Tech. Rep. June, Mesoscale and Microscale Meteorology Division. National Center for Atmospheric Research, Boulder, Colorado, USA. http://dx.doi.org/10.5065/D6DZ069T.

Srinivas, C., Venkatesan, R., 2012. Regional scale atmospheric dispersion simulation of accidental releases of radionuclides from Fukushima Daiichi reactor. Atmos. Environ. 61, 66–84. http://dx.doi.org/10.1016/j.atmosenv.2012.06.082.

Stohl, A., Forster, C., Frank, A., Seibert, P., Wotawa, G., 2005. Technical note: the Lagrangian particle dispersion model FLEXPART version 6.2. Atmos. Chem. Phys. 5 (9), 2461–2474. http://dx.doi.org/10.5194/acp-5-2461-2005.

Stohl, A., Seibert, P., Wotawa, G., Arnold, D., Burkhart, J.F., Eckhardt, S., Tapia, C., Vargas, A., Yasunari, T.J., 2012. Xenon-133 and Caesium-137 releases into the atmosphere from the Fukushima Daiichi nuclear power plant: determination of the source term, atmospheric dispersion. Atmos. Chem. Phys. 12 (5), 2313–2343. http://dx.doi.org/10.5194/acp-12-2313-2012.

Terada, H., Katata, G., Chino, M., Nagai, H., 2012. Atmospheric discharge and dispersion of radionuclides during the Fukushima Daiichi Nuclear Power Plant accident. Part II: verification of the source term. J. Environ. Radioact. 112, 141–154. http://dx.doi.org/10.1016/j.jenvrad. 2012.05.023.

Uppala, S.M., Kållberg, P.W., Simmons, A.J., Andrae, U., Bechtold, V.D.C., Fiorino, M., Gibson, J.K., Haseler, J., Hernandez, A., Kelly, G.A., Li, X., Onogi, K., Saarinen, S., Sokka, N., Allan, R.P., Andersson, E., Arpe, K., Balmaseda, M.A., Beljaars, A.C.M., Berg, L.V.D., Bidlot, J., Bormann, N., Caires, S., Chevallier, F., Dethof, A., Dragosavac, M., Fisher, M., Fuentes, M., Hagemann, S., Hólm, E., Hoskins, B.J., Isaksen, L., Janssen, P.A.E.M., Jenne, R., McNally, A.P., Mahfouf, J.-F., Morcrette, J.-J., Rayner, N.A., Saunders, R.W., Simon, P., Sterl, A., Trenberth, K.E., Untch, A., Vasiljevic, D., Viterbo, P., Woollen, J., 2005. The ERA-40 re-analysis. Q. J. R. Meteorological Soc. 131 (612), 2961–3012. http://dx.doi.org/10.1256/qj.04.176.

Winiarek, V., Bocquet, M., Duhanyan, N., 2014. Estimation of the caesium-137 source term from the Fukushima Daiichi nuclear power plant using a consistent joint assimilation of air concentration and deposition. Atmos. Environ. 82, 268–279. http://dx.doi.org/10.1016/j.atmosenv.2013.10.017.